In vitro generated extracellular matrix and fluid shear stress synergistically enhance 3D osteoblastic differentiation

Néha Datta[†‡], Quynh P. Pham[†‡], Upma Sharma[†‡], Vassilios I. Sikavitsas[§], John A. Jansen[¶], and Antonios G. Mikos[†‖]

[†]Department of Bioengineering, Rice University, MS-142, P.O. Box 1892, Houston, TX 77251-1892; [§]School of Chemical, Biological, and Materials Engineering, University of Oklahoma, 100 East Boyd, T-335, Norman, OK 73019; and [¶]Department of Periodontology and Biomaterials, Radboud University Nijmegen Medical Center, P.O. Box 9101, 6500 HB, Nijmegen, The Netherlands

Edited by Robert Langer, Massachusetts Institute of Technology, Cambridge, MA, and approved December 30, 2005 (received for review July 8, 2005)

This study instituted a unique approach to bone tissue engineering by combining effects of mechanical stimulation in the form of fluid shear stresses and the presence of bone-like extracellular matrix (ECM) on osteodifferentiation. Rat marrow stromal cells (MSCs) harvested from bone marrow were cultured on titanium (Ti) fiber mesh discs for 12 days in a flow perfusion system to generate constructs containing bone-like ECM. To observe osteodifferentiation and bone-like matrix deposition, these decellularized constructs and plain Ti fiber meshes were seeded with MSCs (Ti/ECM and Ti, respectively) and cultured in the presence of fluid shear stresses either with or without the osteogenic culture supplement dexamethasone. The calcium content, alkaline phosphatase activity, and osteopontin secretion were monitored as indicators of MSC differentiation. Ti/ECM constructs demonstrated a 75-fold increase in calcium content compared with their Ti counterparts after 16 days of culture. After 16 days, the presence of dexamethasone enhanced the effects of fluid shear stress and the bone-like ECM by increasing mineralization 50-fold for Ti/ECM constructs; even in the absence of dexamethasone, the Ti/ECM constructs exhibited approximately a 40-fold increase in mineralization compared with their Ti counterparts. Additionally, denatured Ti/ECM* constructs demonstrated a 60-fold decrease in calcium content compared with Ti/ECM constructs after 4 days of culture. These results indicate that the inherent osteoinductive potential of bone-like ECM along with fluid shear stresses synergistically enhance the osteodifferentiation of MSCs with profound implications on bone-tissue-engineering applications.

bone tissue engineering | marrow stromal cells | flow perfusion | bioreactor

Despite the innate ability of bone to heal, there are still approximately one million bone-substitute operations performed annually in the United States alone (1). Current treatments for osseous defects and anomalies include the use of autografts, allografts, and metallic implants (2). However, the limited availability and donor-site morbidity of autografts and issues with immune responses from allografts and metallic implants are drawbacks to these methods (3, 4). The need for osteogenic bone substitutes has led to the development of many bone tissue engineering strategies. By combining different components of the tissue-engineering paradigm (biomaterial scaffolds, cells, and bioactive molecules), the conditions of normal tissue development *in vivo* may be mimicked to recreate functional and structural tissues *in vitro* (5).

An ideal bone tissue engineering scaffold would be both osteoconductive and osteoinductive. Osteoconductivity refers to a scaffold's ability to support osteoblast and osteoprogenitor cell attachment and subsequent bone matrix deposition and formation (4, 6). Inorganic compounds, such as calcium phosphates or hydroxyapatite crystals, are often incorporated into scaffolds with a low osteoconductivity, resulting in increased cell attachment (6). Osteoinductivity describes a scaffold that encourages osteogenic precursor cells to differentiate into mature bone-forming cells (7). Many small fractures and defects heal because of the osteoinductivity of natural bone, leading to investigations of demineralized bone as a potential bone tissue engineering scaffold (8). However, in large bone defects, the inherent osteoinductivity of bone may not be sufficient for adequate healing. Thus, a model scaffold would, itself, be capable of recruiting stem and osteoprogenitor cells to a bone healing site where they would eventually differentiate into extracellular matrix (ECM)-secreting osteoblasts (7). Other considerations for a tissue engineering scaffold include mechanical integrity, biodegradability, biocompatibility, and a porosity that would allow for bone-tissue ingrowth (9).

Most tissue engineering scaffolds (i.e., ceramics, metals, and polymers) are only osteoconductive (9–11). One method to incorporate osteoinductive properties into a scaffold is through the inclusion of growth factors or cytokines specific to the desired tissue to be regenerated. Growth factors known to influence bone cells include transforming growth factors (TGFs) (12), insulin-like growth factors (13), bone morphogenetic proteins (BMPs) (14), fibroblast growth factors (FGFs), and platelet-derived growth factors (15). These critical mediators of bone function regulate the phenotype of osteoblasts and other bone cells by binding to cell-surface receptors, which, in turn, activate cellular responses such as proliferation and differentiation (16).

Marrow stromal cells (MSCs) are multipotent cells found predominantly within the bone marrow that are undifferentiated but, when given the proper environmental cues, can potentially differentiate into various tissue types including but not limited to bone, cartilage, and adipose (17). *In vivo*, osteodifferentiation is marked by sequential stages of cellular proliferation, bone ECM maturation, and matrix mineralization (18). This progression is mediated by cell–growth factor, cell–cell, and cell–matrix interactions (19). Mechanical strain and fluid shear stress have also been demonstrated to influence osteodifferentiation, with load-induced fluid shear stress being shown to have greater effects (20–22). *In vivo*, bone cells experience interstitial fluid shear stress upon mechanical loading of bone through fluid flow inside the canalicular–lacunar and trabecular spaces within bone tissue (23). To accurately mimic the *in vivo* matrix architecture, cells should be cultured in a 3D environment with the appropriate mechanical stimulation.

Bioreactors provide a means to expose cells to dynamic culture conditions *in vitro* (24, 25). An approach used previously in our group focuses on the use of fluid shear stresses generated by a flow perfusion bioreactor to influence osteodifferentiation of

---

Conflict of interest statement: No conflicts declared.

This paper was submitted directly (Track II) to the PNAS office.

Abbreviations: ALP, alkaline phosphatase; ECM, extracellular matrix; GAG, glycosaminoglycan; MSC, marrow stromal cells; SEM, scanning EM.

[‡]N.D., Q.P.P., and U.S. contributed equally to this work.

[‖]To whom correspondence should be addressed. E-mail: mikos@rice.edu.

www.pnas.org/cgi/doi/10.1073/pnas.0505661103

MSCs. We have shown that fluid flow not only mitigates nutrient transport limitations in 3D perfusion cultures of MSCs but also provides mechanical stimulation to seeded cells in the form of fluid shear stress, resulting in increased depositions of mineralized matrix (26, 27). Cellular constructs cultured in a flow perfusion bioreactor yielded a significant increase in matrix mineralization after 16 days as compared with those cultured statically when cultured in the presence of osteogenic supplements, including dexamethasone, which has been shown to be a powerful promoter of osteodifferentiation (28). Furthermore, flow perfusion culture in the absence of dexamethasone resulted in more mineralization than static culture in the presence of dexamethasone (29). These results indicated that fluid shear stresses can positively influence and enhance osteodifferentiation of MSCs on porous scaffolds.

In vivo, the ECM plays an important role in maintaining and mediating bone function. Several studies suggest that the 3D matrix structure and organization can influence the phenotypic behavior of cells (1, 30). Native bone is a highly dynamic and complex system that consists predominately of a mineralized ECM secreted by osteoblasts (31). The organic components of bone-like ECM are composed of 90% type I collagen, whereas the remaining 10% consists of noncollagenous proteins (32, 33). The ECM contains various osteoinductive factors, as evidenced by bone formation in ectopic sites using demineralized bone (34). Located throughout the bone matrix are a variety of glycoproteins, such as thrombospondin, fibronectin, vitronectin, and fibrillin, which help promote cellular attachment (32). Mechanical signals are conveyed through these adhesion proteins to attached cells and cause changes in gene expression and phenotype (35). Osteopontin, bone sialoprotein, and other matrix glycoproteins are also involved in the matrix mineralization processes (33). To capitalize on the beneficial properties of ECM, we have cultured MSCs on titanium (Ti) scaffolds to generate bone-like ECM *in vitro*. The presence of this bone-like ECM resulted in significantly larger mineral deposition by MSCs over 16 days under static culture conditions as compared with constructs without pregenerated ECM (36). These results suggested that the presence of the pregenerated bone-like ECM transformed the Ti scaffold from an osteoconductive to an osteoinductive construct.

In this work, we aimed to combine the beneficial properties of fluid shear stress with those of pregenerated ECM. To do so, MSCs were seeded onto either plain Ti or pregenerated ECM-containing Ti meshes and cultured in a flow perfusion bioreactor. A comparison of these constructs enabled us to examine the osteoinductive potential of an *in vitro* pregenerated ECM on osteoblast differentiation in the presence of fluid shear stresses. Because plain Ti constructs and those containing pregenerated ECM have different pore sizes (the ECM fills the void volume of the plain Ti scaffold), fluid flow through each of these constructs will exert different shear stresses on the seeded cells. To separate the effects of the *in vitro* generated ECM from those due to differences in shear stress, a group of constructs containing denatured pregenerated ECM were fabricated; doing so allowed for the effects of the generated ECM to be measured directly. Finally, to elucidate its osteogenic effect, the 3D *in vitro* culture of such constructs was carried out either with or without dexamethasone in the culture media. Known markers of differentiation, including expression of alkaline phosphatase (ALP), secretion of osteopontin, and deposition of a calcified ECM were used as indicators of cell differentiation and mineralization. Our approach combines all three elements of the tissue engineering paradigm: MSCs capable of osteodifferentiation, Ti fiber mesh as an osteoconductive scaffold, and a pregenerated bone-like ECM as a source of bone cell differentiation supporting factors.

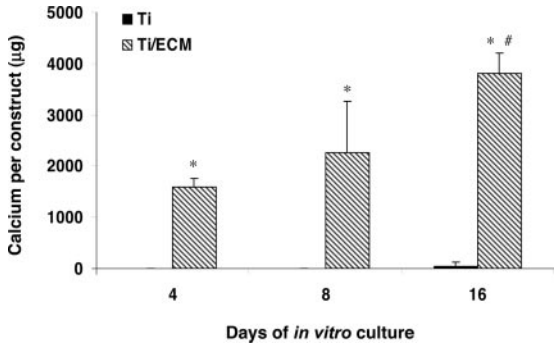

Fig. 1. The calcium content of Ti and Ti/ECM constructs cultured in the flow-perfusion bioreactor after 4, 8, and 16 days of culture. The data represent means of four samples, with the error bars representing the standard deviations. Statistical differences ($P < 0.05$) between Ti and Ti/ECM constructs are indicated with an asterisk; # designates a statistical difference ($P < 0.05$) between all other data points.

Results and Discussion

This study investigated the osteoinductive capacity of an *in vitro* pregenerated ECM on the proliferation and differentiation of marrow stromal cells seeded on 3D Ti fiber mesh scaffolds and cultured in a flow-perfusion bioreactor. The pregenerated ECM used in this study was secreted by MSCs over a 12-day culture period to allow for sufficient matrix deposition; compositional analysis of the matrix indicated the presence of glycosaminoglycans (GAGs) and collagen (as determined by biochemical analysis of the Ti/ECM constructs) (see Fig. 5, which is published as supporting information on the PNAS web site). The specific questions we wanted to answer were: (*i*) What effect does the combination of bone-like ECM and flow have on osteodifferentiation? (*ii*) How is this effect different in the presence and absence of the osteogenic culture supplement dexamethasone?

Because the endpoint of osteoblast phenotypic expression is indicated by the production of a calcified, mineralized matrix (37), we measured the calcium content in the constructs as an indicator of osteodifferentiation. The measured calcium content increased with time for both Ti and Ti/ECM constructs (Fig. 1). Ti constructs, when cultured under flow perfusion in the presence of dexamethasone for 16 days, contained ≈50 μg of calcium. In contrast, the Ti/ECM constructs yielded 75 times more calcium after the same amount of time, ≈3,800 μg. After only 4 days of culture, the calcium content of the Ti/ECM constructs was already ≈1,600 μg, whereas only 2 μg were observed in Ti constructs.

The substantial increase in calcium content after only 4 days in Ti/ECM constructs could be attributed to two things: (*i*) the presence of the ECM in the Ti/ECM constructs and (*ii*) differences in the shear stress exerted on the cells in these constructs compared with plain Ti constructs. A previously developed cylindrical pore model showed that the fluid shear stress exerted on cells in a scaffold depends on the pore size of the construct: for a given flow rate, MSCs on constructs with smaller pore sizes experience larger shear stress and subsequently demonstrate greater matrix mineralization (38). Mercury porosimetry measurements confirmed a difference in the pore sizes of Ti and Ti/ECM scaffolds (65.3 ± 3.0 μm versus 29.8 ± 7.1 μm, respectively), which could explain the increased mineralization in Ti/ECM scaffolds.

To separate the effects of the pore-size differences between the Ti and Ti/ECM groups from the impact of the ECM, some Ti/ECM scaffolds were denatured by heat treatment to deactivate the growth factors contained within the *in vitro* generated ECM. These Ti/ECM* constructs had an average pore size that was not significantly different from Ti/ECM constructs (29.8 ±

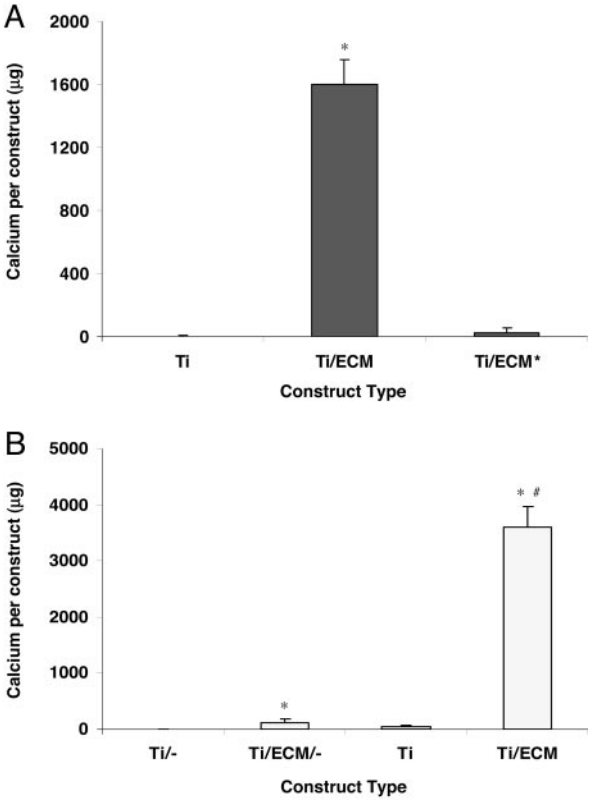

Fig. 2. Calcium content of constructs cultured in the flow-perfusion bioreactor. (*A*) The calcium content of Ti, Ti/ECM, and Ti/ECM* constructs after four days of culture. (*B*) The calcium content of Ti and Ti/ECM constructs cultured in the presence and absence (−) of dexamethasone after 16 days. The data represent means of four samples, with the error bars representing the standard deviations. Statistical differences ($P < 0.05$) between constructs are indicated with an asterisk; # designates a statistical difference ($P < 0.05$) between all other data points.

7.1 versus 25.7 ± 4.6 μm, respectively). Nevertheless, Ti/ECM* constructs demonstrated significantly less calcium than Ti/ECM constructs after 4 days of culture (27 μg and 1,600 μg, respectively) (Fig. 2*A*). The Ti/ECM* constructs had greater cellularity than Ti and Ti/ECM constructs, indicating that the cells were able to attach and proliferate on these scaffolds (data not shown). Therefore, we hypothesize that the increased matrix mineralization observed on Ti/ECM constructs compared with Ti/ECM* is an indicator of enhanced osteodifferentiation of MSCs on the Ti/ECM constructs because of the bioactive growth factors present in the pregenerated matrix; in the heat-treated Ti/ECM* constructs, these growth factors were not active, and, therefore, less osteodifferentiation was observed.

The role of dexamethasone in these substantial increases of mineral content was examined by comparing calcium data for the Ti/ECM/- and Ti/- constructs in flow perfusion to those constructs cultured in the presence of dexamethasone (Ti/ECM and Ti). After 16 days of culture, Ti/ECM/- constructs contained ≈75 μg of calcium, and the Ti/- constructs had ≈1 μg of Ca (Fig. 2*B*). Because the mineralized matrix deposition in both ECM containing groups (Ti/ECM and Ti/ECM/-) was significantly higher than their counterparts (Ti and Ti/-), there was a stimulatory effect of the pregenerated ECM on MSCs. Furthermore, even in the absence of dexamethasone, the calcium content in the Ti/ECM/- constructs after 16 days of culture was greater than in the Ti constructs, lending further credence to the osteoinductive capability of the bone-like ECM.

Furthermore, the results of this study were compared with a study in which Ti/ECM constructs were cultured statically (36) to isolate the effects of the pregenerated ECM from those of flow-perfusion culture. The calcium content of the Ti/ECM constructs in this study demonstrated a 5-fold increase relative to corresponding static Ti/ECM constructs of the previous study. For plain Ti constructs, only a 2-fold increase was observed for flow culture as compared with static culture. These results indicate that the combination of the pregenerated bone-like ECM and flow-perfusion culture in the presence of dexamethasone synergistically impact the differentiation of MSCs.

The calcium data were corroborated by examining the constructs by using scanning (S)EM and energy dispersive spectroscopy (EDS). Before *in vitro* culture, cells were seeded on the top of the scaffolds, resulting in more cells and ECM at the top of the scaffolds initially (see Fig. 6, which is published as supporting information on the PNAS web site). Images of the tops and bottoms of Ti and Ti/ECM constructs were obtained at 0, 4, 8, and 16 days to follow the evolution of the ECM deposition and matrix mineralization throughout the construct. Extensive mineralization (composed of calcium and phosphorous, according to EDS analysis) was observed at the top surfaces of Ti/ECM scaffolds after 4, 8, and 16 days of culture; by day 16, the Ti fibers were encased in ECM and no longer visible on either side of the construct.

Additionally, cross-sections of the constructs were cut and analyzed by SEM to examine the distribution of ECM throughout the constructs. Fig. 3 shows SEM images of a Ti construct after 16 days of culture (Fig. 3*A*), a Ti/ECM construct after 4 days of culture (Fig. 3*B*), and a Ti/ECM construct after 16 days of culture (Fig. 3*C*). After 16 days of flow culture, it is evident that ECM is distributed throughout Ti constructs; however, void spaces are still visible, and little mineralization is observed. In contrast, there are few open spaces in the Ti/ECM constructs after the same amount of time because of the presence of a substantial amount of mineralized matrix (Fig. 3*C*). Furthermore, a direct comparison of a Ti construct cultured for 16 days (Fig. 3*A*) and a Ti/ECM construct cultured for 4 days (Fig. 3*B*) provides a qualitative appreciation for the impact of preexisting ECM. (The Ti/ECM construct is pregenerated with a 12-day culture period, so the total *in vitro* culture period under flow perfusion is 16 days for both cases.) These results indicate that the presence of ECM and flow leads to enhanced mineralization and more uniform matrix distribution.

Before matrix mineralization, osteodifferentiation is marked by sequential stages of cellular proliferation and bone ECM maturation (18). As a measure of proliferation, the cellularities of the Ti and Ti/ECM constructs were measured (see Fig. 7, which is published as supporting information on the PNAS web site). In both groups, the cellularities exhibited a peak at day 8 accompanied by a fall by day 16. The decrease in cellularity of constructs between days 8 and 16 can be attributed to the fact that higher matrix deposition and mineralization with time cause cells to become encased within the matrix and, hence, not detected by the DNA assay. Additionally, the Ti/ECM constructs had significantly lower cellularities at days 8 and 16 compared with Ti constructs, which could be an indication of poor cell proliferation or cell death in the interior of these scaffolds. However, the presence of extensive mineralized matrix indirectly suggests that the cells were viable and continued to deposit matrix. An alternative explanation is that, because Ti/ECM constructs contain more matrix, the lower cell numbers are a result of more cells being encased. As suggested by the calcium data, we hypothesize that MSCs seeded on Ti/ECM constructs interacted with the pregenerated ECM and began to differentiate down the osteoblastic lineage.

This theory is further supported by the measurement of changes in the expression of osteoblastic markers. Specifically, ALP expression is known to peak after the end of the prolifer-

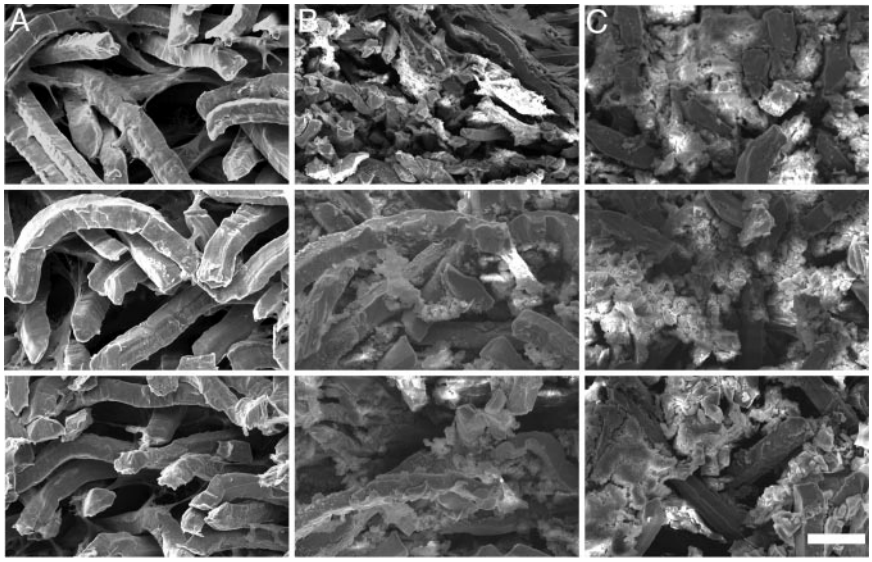

Fig. 3. SEM images obtained from the cross-sections of constructs cultured *in vitro* in a flow-perfusion bioreactor. Each image consists of three panels. (*Top*) One-hundred micrometers from the top of the construct. (*Middle*) The middle of the construct. (*Bottom*) One-hundred micrometers from the bottom surface. These images show the plain Ti construct after 16 days of culture (*A*), the Ti/ECM construct after 4 days of culture (*B*), and the Ti/ECM construct after 16 days of culture (*C*). (Scale bar, 50 μm for all SEM images.)

ative stage and before matrix maturation during osteoblastic differentiation (39). For both Ti and Ti/ECM constructs, there was an increase and then a decrease in ALP activity, with a peak occurring between 4 and 16 days of culture, suggesting that osteodifferentiation was occurring (Fig. 4). Additionally, at each time point, the ALP activity is significantly higher for the Ti/ECM constructs as compared with the Ti constructs. For example, at day 8, the ALP activity of the Ti/ECM constructs is ≈3-fold higher than the Ti constructs. The increased ALP activity in the Ti/ECM constructs indicates that the presence of the bone-like ECM enhances MSC differentiation toward osteoblast-like cells.

In accordance with the ALP activity, we expected the presence of pregenerated bone-like ECM to cause the cells to secrete more osteopontin. Our results, however, demonstrate higher cumulative osteopontin secretions in the Ti constructs as compared with Ti/ECM after 7 days of culture (data shown in Fig. 8, which is published as supporting information on the PNAS web site). In light of the ALP activity of the Ti/ECM constructs, it is likely that osteopontin secretion is underestimated for these samples. We attribute this underestimation to the fact that osteopontin is a calcium-binding protein and will, therefore, be sequestered within the mineralized matrix of the Ti/ECM constructs (36). Additionally, the mineralized matrix will prevent the physical release of osteopontin.

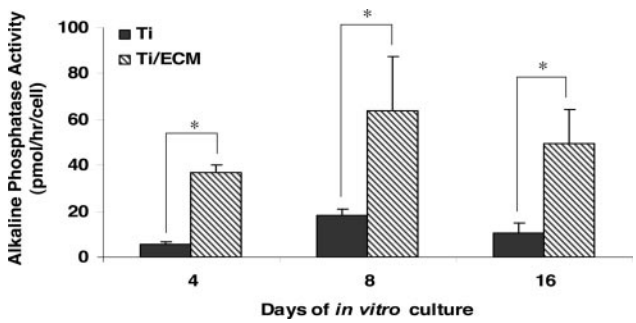

Fig. 4. ALP activity of Ti and Ti/ECM constructs after 4, 8, or 16 days of culture under flow perfusion. The data represent means of four samples, with the error bars representing the standard deviations. Statistical differences ($P < 0.05$) between Ti and Ti/ECM constructs are indicated with an asterisk.

The potential implications of this study on tissue-engineering applications are profound. This approach provides a means to mimic the *in vivo* extracellular environment by using *in vitro* culture. Typical bone tissue engineering scaffolds, such as collagen type I (40), ceramics (10), and demineralized bone (41), contain only the organic or inorganic component of bone and are not representative of native ECM. Composite scaffolds consisting of both phases of bone may represent the overall composition of bone but do not accurately mimic the complexities of bone ECM. Furthermore, there are also considerable limitations with the ability to incorporate multiple bioactive molecules in an optimal configuration for development of bone. Our strategy for bone tissue engineering is to incorporate *in vitro* pregenerated ECM into a scaffold to capitalize on its inherent benefits. The pregenerated ECM in this study contained ≈40 μg of calcium. The presence of calcium phosphate within the matrix alters the chemical composition and surface roughness of the Ti fiber mesh, which can affect the attachment of osteoblast-like cells (42) and adsorption of cytokines and growth factors (43–45). In addition to calcium, we have shown that ECM generated by using a flow perfusion bioreactor contains bone signaling molecules, such as BMP-2, FGF-2, vascular endothelial growth factor, and TGF-β1 (see Fig. 9, which is published as supporting information on the PNAS web site) (46). Although the effects of decellularization on this pregenerated ECM and the contained biomolecules are unknown, the enhanced matrix mineralization observed in Ti/ECM constructs as compared with plain Ti indicates that the ECM retains its osteoinductive nature.

A construct incorporating this pregenerated ECM could thus be implanted into a defect site, where its osteoinductive properties would result in the recruitment of stem and osteoprogenitor cells and adsorption of bioactive molecules within the *in vivo* environment, leading to bone repair and regeneration. Alternatively, the constructs containing pregenerated ECM could be reseeded with autologous MSCs and further cultured *in vitro*

before implantation with two beneficial effects. First, the existing pregenerated ECM contains bioactive molecules that provide signaling cues to direct and enhance MSC differentiation. Second, the *in vitro* 3D flow culture of the Ti/ECM constructs after reseeding leads to an improved distribution of the mineralized matrix throughout the porosity of the scaffolds. This improved distribution is particularly advantageous for tissue-engineering applications; an ideal implant would be able interact with its 3D environment rather than in a restricted 2D interface.

Conclusions

This study demonstrated the synergistic effect of *in vitro* pregenerated ECM and fluid flow on the proliferation and differentiation of MSCs seeded on Ti fiber mesh and cultured in a flow-perfusion bioreactor with dexamethasone. The presence of the pregenerated ECM yielded a significant increase in the amount of mineralized matrix deposited in Ti/ECM constructs as compared with denatured Ti/ECM* constructs, demonstrating the osteoinductive capability of the ECM. In addition, Ti/ECM/- constructs also demonstrated significantly higher calcium content than the Ti/- constructs, indicating that, even in the absence of dexamethasone, the ECM induces osteodifferentiation.

In constructs cultured with dexamethasone, after 16 days of flow culture, mineralized matrix was observed throughout the Ti/ECM constructs. Additionally, an increase in ALP activity of the cells in Ti/ECM constructs was observed. Both ALP and calcium content are indicative of increased osteodifferentiation, indicating that Ti/ECM constructs have increased osteodifferentiation compared with Ti constructs. Also, the mineral content in the Ti/ECM constructs cultured under flow perfusion was 5-fold larger than measured for Ti/ECM constructs cultured statically, indicating a synergistic effect between the bone-like ECM and fluid flow. These results highlight the potential of pregenerated bone-like ECM as a viable scaffold for tissue-engineering applications.

Materials and Methods

Scaffold Preparation. Ti fiber meshes (Bekaert, Zwevegem, Belgium) with porosity of 86% and fiber diameter of 20 μm were die-punched into 8-mm diameter discs (thickness, 0.8 mm). Scaffolds were sterilized by autoclaving before use (26).

Rat MSC Isolation. MSCs were harvested and pooled from 10 male Wistar rats weighing 150–175 g according to established protocols (36). Cells were cultured in the presence of 10^{-8} M dexamethasone for 6 days in complete osteogenic media containing minimum essential media (α modification), 10 mM β-glycerophosphate, 50 μg/ml ascorbic acid, (all from Sigma), and 10% (vol) FBS (Gemini Bio-Products, Woodland, CA). Cells were trypsinized on day 6, suspended in 10% (vol) dimethyl sulfoxide (Sigma) in FBS, aliquoted in 1.5-ml cryovials, placed in a freezing canister overnight at −80°C, and then transferred to liquid nitrogen until use. For constructs cultured without dexamethasone, all procedures were identical, except that dexamethasone was omitted from the media.

Experimental Design. To generate the bone-like ECM, plain Ti meshes were first seeded with MSCs and cultured in complete media under flow for a period of 12 days, after which they were decellularized (36) and sterilized with ethylene oxide gas for 12 h. To remove residual ethylene oxide, the meshes were subsequently aerated for at least 6 h. Ti constructs either with or without pregenerated ECM (Ti and Ti/ECM constructs, respectively) were prewet in PBS for 1 h and then seeded with MSCs and cultured in a flow-perfusion bioreactor for 4, 8, or 16 days. Additionally, denatured Ti/ECM constructs (Ti/ECM*) were obtained by exposing Ti/ECM constructs to heat; these Ti/ECM* constructs were subsequently seeded with MSCs and cultured in complete media under flow for 4 days. To study matrix mineralization in the absence of dexamethasone, Ti and Ti/ECM constructs were also seeded with MSCs and cultured in the absence of dexamethasone for 16 days; these groups are represented as Ti/- and Ti/ECM/- constructs.

Flow Perfusion Culture of MSCs on Ti Meshes. The flow perfusion culture system was set up as described in detail by Bancroft *et al.* (24). Plain Ti fiber meshes were seeded with 250,000 MSCs in 200 ml of complete media to generate Ti constructs. After 2 days, the cassettes containing the seeded constructs were placed in the bioreactor. The operation of the bioreactor system was driven by a peristaltic pump set at a rate of 1 ml/min. The cells were cultured in complete media for 4, 8, or 16 days, with a complete media exchange every 48 h. Each group consisted of six samples, including one for SEM analysis. At the end of the culture period, all constructs were rinsed with PBS and stored in 1.5 ml of distilled, deionized water at −20°C until further use.

Ti/ECM Construct Generation. Cryopreserved MSCs were resuscitated in complete osteogenic media and subsequently cultured for 6 days. Ti meshes were seeded as described above. The constructs were cultured for 12 days in the flow-perfusion bioreactor in complete medium. At the end of the culture period, constructs were rinsed and stored in distilled, deionized water at −20°C.

To remove cellular components, the meshes were decellularized by using three consecutive freeze–thaw cycles (47), resulting in constructs that have been shown to contain no cells (36). The Ti/ECM constructs were allowed to air dry, sterilized with ethylene oxide, and then press-fit into flow-system cassettes in a six-well plate for further culture in the bioreactor, as previously described. Preparation of Ti/ECM* constructs was performed in a similar manner, except that, immediately after decellularization, the Ti/ECM meshes were placed in a 70°C water bath for 5 min.

Mercury Porosimetry. Scaffold pore size was measured by using mercury porosimetry (Autoscan 500, Quantachrome Instruments, Boynton Beach, FL) as described in ref. 38. Scaffolds were placed into the sample chamber, and the void space in the chamber was filled with mercury. The pressure was then increased at a rate of 0.01 psi/s until a total pressure of 50 psi was reached. Volume versus pressure data were converted to pore size by using software supplied by the vendor (Quantachrome Instruments AUTOSCAN, ver. 3.00). Measurements were made on three samples of each scaffold type.

SEM Analysis. Samples were fixed in 2.5% (vol) glutaraldehyde for 2 h. The samples were cut in half for analysis of both the top and bottom; additionally, a cross-section was cut. All samples were dried, mounted on aluminium stages, sputter coated with gold, and examined with an FEI-XL 30 Environmental Scanning Electron Microscope; energy dispersive spectroscopy (EDAX, Mahwah, NJ) was performed in conjunction with the SEM imaging.

Biochemical Assays. The cellularity and ALP enzyme activity of the constructs were determined as described in ref. 36. Briefly, Ti constructs were sonicated for 10 min. The DNA of the supernatant was quantified by using the PicoGreen assay (Molecular Probes) and compared with DNA extracted from known numbers of MSCs. ALP enzyme activity of the constructs was measured by using the supernatant and the Alkaline Phosphatase Assay from Sigma. Calcium content of the constructs was determined by using a calcium quantification assay obtained from Diagnostic Chemicals (Charlottetown, PEI, Canada) as

described in ref. 29. After the DNA and ALP assays were performed, the constructs were placed in acetic acid (0.5 N) overnight to dissolve calcium. For all Ti/ECM and Ti/ECM* constructs, the calcium present in the initial decellularized construct (≈40 μg) was accounted for.

To determine the total collagen and GAG content of the Ti/ECM constructs, constructs were first cut into fine pieces with scissors and then digested with proteinase K solution (1 mg/ml proteinase K, 10 μg/ml pepstatin A, and 185 μg/ml iodoacetamide) in phosphate-buffered EDTA [6.055 mg/ml Tris (hydroxymethyl aminomethane) and 0.372 mg/ml EDTA, pH 7.6, adjusted by HCl] for 16 h in a 56°C water bath. An aliquot of the solution after digestion was used to perform the dimethylmethylene blue dye assay to determine the GAG content in each construct as described in ref. 48. Total collagen content was performed after a hydroxyproline assay of an aliquot of the digested samples. Briefly, 200 ml of the digested sample was hydrolyzed in 6 M HCl for 4 h at 115°C. Samples were allowed to cool to room temperature and the HCl evaporated under nitrogen flow. The hydrolyzate was dissolved in 700 ml of distilled, deionized H_2O and then a sample was mixed with chloramine-T solution and *p*-dimethylaminobenzaldehyde (49). The absorbance was read by using a plate reader at a wavelength of 570 nm. Collagen content was determined, following a 1:10 ratio of hydroxyproline to collagen (50).

Osteopontin Assay. Osteopontin content of the constructs was measured by using an ELISA kit against rat osteopontin available from Assay Designs (Ann Arbor, MI) as described in ref. 36. Media samples were collected every 2 days during the culture period and stored at −20°C. Samples were run in duplicate and compared against rat osteopontin standards.

Statistical Analysis. Samples for DNA, ALP, and calcium assays were performed in triplicate and results reported as means ± standard deviation for four different scaffolds. Osteopontin secretion was determined from a media sample that represented a pool of six samples; the assay for osteopontin was performed in duplicate. A two-factor repeated-measures ANOVA was performed before making multiple comparisons among Ti, Ti/ECM, Ti/-, and Ti/ECM/- constructs by using the Tukey procedure at a significance level of 95%. A one-way ANOVA was performed before comparing means among Ti, Ti/ECM, and Ti/ECM* constructs by using the Tukey procedure at a significance level of 95%. Statistical analysis of total collagen and GAG content was performed similarly for three different scaffolds.

We thank Professor Jane K. Grande-Allen (Rice University) for her assistance with the collagen and GAG analysis of the constructs. This work was supported by National Institutes of Health (NIH) Grant R01-AR42639 (to A.G.M.). U.S. acknowledges support from a training fellowship from the Keck Center Nanobiology Training Program of the Gulf Coast Consortia (NIH Grant 1 T90 DK070121-01).

1. Salgado, A. J., Coutinho, O. P. & Reis, R. L. (2004) *Macromol. Biosci.* **4,** 743–765.
2. Hatano, H., Ogose, A., Hotta, T., Endo, N., Umezu, H. & Morita, T. (2005) *J. Bone Jt. Surg. Br. Vol.* **87,** 1006–1011.
3. Fodor, W. L. (2003) *Reprod. Biol. Endocrinol.* **1,** 102.
4. Kofron, M. D., Li, X. & Laurencin, C. T. (2004) *Curr. Opin. Biotechnol.* **15,** 399–405.
5. Li, W. J., Tuli, R., Huang, X., Laquerriere, P. & Tuan, R. S. (2005) *Biomaterials* **26,** 5158–5166.
6. LeGeros, R. Z. (2002) *Clin. Orthop. Relat. Res.*, 81–98.
7. Burg, K. J., Porter, S. & Kellam, J. F. (2000) *Biomaterials* **21,** 2347–2359.
8. Hofmann, A., Konrad, L., Gotzen, L., Printz, H., Ramaswamy, A. & Hofmann, C. (2003) *J. Biomed. Mater. Res. A* **67,** 191–199.
9. Liu, X. & Ma, P. X. (2004) *Ann. Biomed. Eng.* **32,** 477–486.
10. Knabe, C., Driessens, F. C., Planell, J. A., Gildenhaar, R., Berger, G., Reif, D., Fitzner, R., Radlanski, R. J. & Gross, U. (2000) *J. Biomed. Mater. Res.* **52,** 498–508.
11. Vehof, J. W., van den Dolder, J., de Ruijter, J. E., Spauwen, P. H. & Jansen, J. A. (2003) *J. Biomed. Mater. Res. A* **64,** 417–426.
12. Ong, J. L., Carnes, D. L. & Sogal, A. (1999) *Int. J. Oral Maxillofacial Implants* **14,** 217–225.
13. Rosen, C. J. (2004) *Best Pract. Res. Clin. Endocrinol. Metab.* **18,** 423–435.
14. Kroese-Deutman, H. C., Ruhe, P. Q., Spauwen, P. H. & Jansen, J. A. (2005) *Biomaterials* **26,** 1131–1138.
15. Parikh, S. N. (2002) *J. Postgrad. Med.* **48,** 142–148.
16. Mistry, A. S. & Mikos, A. G. (2005) *Adv. Biochem. Eng. Biotechnol.* **94,** 1–22.
17. Tondreau, T., Lagneaux, L., Dejeneffe, M., Massy, M., Mortier, C., Delforge, A. & Bron, D. (2004) *Differentiation (Berlin)* **72,** 319–326.
18. Quarles, L. D., Yohay, D. A., Lever, L. W., Caton, R. & Wenstrup, R. J. (1992) *J. Bone Miner. Res.* **7,** 683–692.
19. Shin, H., Temenoff, J. S., Bowden, G. C., Zygourakis, K., Farach-Carson, M. C., Yaszemski, M. J. & Mikos, A. G. (2005) *Biomaterials* **26,** 3645–3654.
20. Owan, I., Burr, D. B., Turner, C. H., Qiu, J., Tu, Y., Onyia, J. E. & Duncan, R. L. (1997) *Am. J. Physiol. C* **273,** 810–815.
21. Tanaka, S. M., Sun, H. B., Roeder, R. K., Burr, D. B., Turner, C. H. & Yokota, H. (2005) *Calcif. Tissue Int.* **76,** 261–271.
22. You, J., Yellowley, C. E., Donahue, H. J., Zhang, Y., Chen, Q. & Jacobs, C. R. (2000) *J. Biomech. Eng.* **122,** 387–393.
23. Norvell, S. M., Alvarez, M., Bidwell, J. P. & Pavalko, F. M. (2004) *Calcif. Tissue Int.* **75,** 396–404.
24. Bancroft, G. N., Sikavitsas, V. I. & Mikos, A. G. (2003) *Tissue Eng.* **9,** 549–554.
25. Yu, X., Botchwey, E. A., Levine, E. M., Pollack, S. R. & Laurencin, C. T. (2004) *Proc. Natl. Acad. Sci. USA* **101,** 11203–11208.
26. Bancroft, G. N., Sikavitsast, V. I., van den Dolder, J., Sheffield, T. L., Ambrose, C. G., Jansen, J. A. & Mikos, A. G. (2002) *Proc. Natl. Acad. Sci. USA* **99,** 12600–12605.
27. Sikavitsas, V. I., Bancroft, G. N., Holtorf, H. L., Jansen, J. A. & Mikos, A. G. (2003) *Proc. Natl. Acad. Sci. USA* **100,** 14683–14688.
28. van den Dolder, J., Bancroft, G. N., Sikavitsas, V. I., Spauwen, P. H., Jansen, J. A. & Mikos, A. G. (2003) *J. Biomed. Mater. Res. A* **64,** 235–241.
29. Holtorf, H. L., Jansen, J. A. & Mikos, A. G. (2005) *J. Biomed. Mater. Res. A* **72,** 326–334.
30. Cukierman, E., Pankov, R., Stevens, D. R. & Yamada, K. M. (2001) *Science* **294,** 1708–1712.
31. Endres, M., Hutmacher, D. W., Salgado, A. J., Kaps, C., Ringe, J., Reis, R. L., Sittinger, M., Brandwood, A. & Schantz, J. T. (2003) *Tissue Eng.* **9,** 689–702.
32. Robey, P. G. (2002) in *Principles of Bone Biology*, eds. Biliezikian, J. P., Raisz, L. G. & Rodan, G. A., Vol. 1, pp. 225–237.
33. Riminucci, M. & Bianco, P. (2003) *Braz. J. Med. Biol. Res.* **36,** 1027–1036.
34. Service, R. F. (2000) *Science* **289,** 1498–1500.
35. Rosso, F., Marino, G., Giordano, A., Barbarisi, M., Parmeggiani, D. & Barbarisi, A. (2005) *J. Cell. Physiol.* **203,** 465–470.
36. Datta, N., Holtorf, H. L., Sikavitsas, V. I., Jansen, J. A. & Mikos, A. G. (2005) *Biomaterials* **26,** 971–977.
37. Lian, J. B. & Stein, G. S. (1992) *Crit. Rev. Oral Biol. Med.* **3,** 269–305.
38. Holtorf, H. L., Datta, N., Jansen, J. A. & Mikos, A. G. (2005) *J. Biomed. Mater. Res. A* **74,** 171–180.
39. Owen, T. A., Aronow, M., Shalhoub, V., Barone, L. M., Wilming, L., Tassinari, M. S., Kennedy, M. B., Pockwinse, S., Lian, J. B. & Stein, G. S. (1990) *J. Cell. Physiol.* **143,** 420–430.
40. Rodrigues, C. V., Serricella, P., Linhares, A. B., Guerdes, R. M., Borojevic, R., Rossi, M. A., Duarte, M. E. & Farina, M. (2003) *Biomaterials* **24,** 4987–4997.
41. Mauney, J. R., Blumberg, J., Pirun, M., Volloch, V., Vunjak-Novakovic, G. & Kaplan, D. L. (2004) *Tissue Eng.* **10,** 81–92.
42. Keller, J. C., Collins, J. G., Niederauer, G. G. & McGee, T. D. (1997) *Dent. Mater.* **13,** 62–68.
43. Dennis, J. E., Haynesworth, S. E., Young, R. G. & Caplan, A. I. (1992) *Cell Transplant.* **1,** 23–32.
44. Laffargue, P., Fialdes, P., Frayssinet, P., Rtaimate, M., Hildebrand, H. F. & Marchandise, X. (2000) *J. Biomed. Mater. Res.* **49,** 415–421.
45. Yuan, H., Zou, P., Yang, Z., Zhang, X., De Bruijn, J. D. & De Groot, K. (1998) *J. Mater. Sci. Mater. Med.* **9,** 717–721.
46. Gomes, M. E., Bossano, C. M., Johnston, C. M., Reis, R. L. & Mikos, A. G. *Tissue Eng.*, in press.
47. Medalie, D. A., Eming, S. A., Collins, M. E., Tompkins, R. G., Yarmush, M. L. & Morgan, J. R. (1997) *Transplantation* **64,** 454–465.
48. Park, H., Temenoff, J. S., Holland, T. A., Tabata, Y. & Mikos, A. G. (2005) *Biomaterials* **26,** 7095–7103.
49. Grande-Allen, K. J., Griffin, B. P., Ratliff, N. B., Cosgrove, D. M. & Vesely, I. (2003) *J. Am. Coll. Cardiol.* **42,** 271–277.
50. Vunjak-Novakovic, G., Martin, I., Obradovic, B., Treppo, S., Grodzinsky, A. J., Langer, R. & Freed, L. E. (1999) *J. Orthop. Res.* **17,** 130–138.